J. Fluid Mech. (1970), *vol.* 41, *part* 2, *pp.* 387–403
Boeing Symposium on Turbulence

Relationship between a Wiener–Hermite expansion and an energy cascade

By S. C. CROW
Boeing Scientific Research Laboratories, Seattle, Washington
AND G. H. CANAVAN
Air Force Weapons Laboratory, Kirtland Air Force Base, New Mexico

(Received 29 August 1969)

Meecham and his co-workers have developed a theory of turbulence involving a truncated Wiener–Hermite expansion of the velocity field. The randomness is taken up by a white-noise function associated, in the original version of the theory, with the initial state of the flow. The mechanical problem then reduces to a set of coupled integro-differential equations for deterministic kernels. We have solved numerically an analogous set for Burgers's model equation and have computed, for the sake of comparison, actual random solutions of the Burgers equation. We find that the theory based on the first two terms of the Wiener–Hermite expansion predicts an insufficient rate of energy decay for Reynolds numbers larger than two, because the equations for the kernels contain no convolution integrals in wave-number space and therefore permit no cascade of energy. An energy cascade in wave-number space corresponds to a cascade up through successive terms of the Wiener–Hermite expansion. Pictures of the Gaussian and non-Gaussian components of an actual solution of the Burgers equation show directly that only higher-order terms in the Wiener–Hermite expansion are capable of representing shocks, which dissipate the energy. Higher-order terms would be needed even for a nearly Gaussian field of evolving three-dimensional turbulence. 'Gaussianity', in the experimentalist's sense, has no bearing on the rate of convergence of a Wiener–Hermite expansion whose white-noise function is associated with the initial state. Such an expansion would converge only if the velocity field and its initial state were joint-normally distributed. The question whether a time-varying white-noise function can speed the convergence is treated in the paper following this one.

1. Introduction

Thirty years ago, Wiener (1939) proposed a novel method for analyzing hydrodynamic turbulence: the turbulent field was to be expanded as a polynomial series in powers of the 'pure chaos', a colourful name for what has since become known as the white-noise function. The idea lay dormant for twenty years, but in the last ten years it has stimulated considerable activity, largely due to the publication of Wiener's (1958) book on non-linear random processes

Printed in Great Britain

and to a series of papers presented by Meecham and his co-workers (Siegel & Meecham 1959, Meecham & Siegel 1964, Meecham & Jeng 1968).

The terms in Wiener's expansion have the form of Hermite polynomials in the white-noise function. In order to see why Hermite polynomials are advantageous, let us consider the case of a single variable y that has evolved in time t from some initial state a. $y(t;a)$ might be the solution of a first-order differential equation under the initial condition $y(0;a) = a$. Under fairly general circumstances, y can be expanded in terms of its initial state as a series of Hermite polynomials

$$y(t;a) = \sum_{n=0}^{\infty} k_n(t)\, h_n(a). \tag{1.1}$$

The $k_n(t)$ are coefficients characterizing the relationship between y and a, and

$$h_n(a) = \frac{(-1)^n}{\sqrt{(n!)}} e^{\frac{1}{2}a^2} \frac{d^n}{da^n} e^{-\frac{1}{2}a^2}.$$

The first few of the Hermite polynomials h_n are as follows:

$$h_0 = 1, \quad h_1 = a, \quad h_2 = (a^2-1)/\sqrt{2}, \quad h_3 = (a^3-3a)/\sqrt{6}, \quad \text{etc.}$$

The h_n have been normalized so that they are orthonormal under the weighting function

$$G(a) = \frac{1}{\sqrt{(2\pi)}} e^{-\frac{1}{2}a^2}.$$

Thus

$$\int_{-\infty}^{\infty} G(a)\, h_m(a)\, h_n(a)\, da = \delta_{mn}.$$

Given a function $y(t;a)$, the corresponding coefficients $k_n(t)$ can be extracted according to the prescription

$$k_n(t) = \int_{-\infty}^{\infty} G(a)\, h_n(a)\, y(t;a)\, da. \tag{1.2}$$

No statistical considerations have been introduced so far; Hermite polynomials are just one among many possible complete sets of functions into which $y(t;a)$ can be expanded.

The feature that distinguishes the Hermite polynomials is that they are orthonormal with respect to a weighting function $G(a)$ that has the form of a Gaussian probability distribution of unit variance. Suppose that a is a Gaussian random variable and that y is a random strictly on account of its dependence on a, as is the case if y evolves according to a deterministic differential equation. Then the Hermite inversion integral (1.2) means the same thing as

$$k_n(t) = \langle h_n(a)\, y(t;a) \rangle,$$

where the angle brackets denote an ensemble average over the a's; as far as the statistics is concerned, t is just a parameter. The k_n's can be extracted as ensemble averages even if the underlying differential equation is unknown. An analytical expression for $y(t;a)$ can be constructed as a Hermite-polynomial series by averaging randomly selected products of $y(t;a)$ and $h_n(a)$, a technique essentially equivalent to evaluating the Hermite inversion integral by a Monte-Carlo

method. Used in that way, the Wiener–Hermite expansion is a tool for analysing the output of systems whose internal mechanism is unknown.

The expansion is put to use differently in turbulence theory. If $y(t;a)$ were to depend almost linearly on its initial state a, then the $n = 1$ term in the expansion (1.1) would dominate all the others, and y itself would be Gaussian. If the series (1.1) converges rapidly around $n = 1$, in other words, then y is nearly Gaussian. A dynamical theory of turbulence can be founded upon the conjecture that the converse is true: if y is nearly Gaussian, then the Hermite expansion of y in terms of its Gaussian random initial value converges rapidly, *regardless of the dynamics that has transformed* $y(0;a)$ *into* $y(t;a)$. We shall return to the case of a single random variable y in §5 and show by example that the conjecture is not necessarily true. We shall show in §§2–4 that the theory of turbulence based upon the conjecture cannot account for one of the fundamental attributes of turbulence—the energy cascade. Orszag & Bissonnette (1967) have discussed other deficiencies of the theory.

The discussion will be carried out in terms of the Burgers equation, a one-dimensional model of the Navier–Stokes equations. The model is used for algebraic simplicity; our conclusions apply with equal force to the three-dimensional problem (Canavan 1969). Rather than a single random variable y, a random *function* $u(x)$ is needed to describe one realization of the model turbulence at a particular time; x is the spatial co-ordinate and u is the velocity. Assuming that u is statistically homogeneous in x, Meecham & Siegel (1964) deduce a Wiener–Hermite expansion for $u(x,t)$,

$$u(x,t) = \int_{-\infty}^{\infty} K^{(1)}(x-\xi)\, H^{(1)}(\xi)\, d\xi + \int_{-\infty}^{\infty}\int_{-\infty}^{\infty} K^{(2)}(x-\xi, x-\eta)\, H^{(2)}(\xi,\eta)\, d\xi d\eta + \ldots, \tag{1.3}$$

a representation analogous to the Hermite-polynomial expansion of $y(t;a)$. The kernels $K^{(n)}$ are functions of time and fully account for the time dependence of u as well as for its statistical properties. The $H^{(n)}$ are time-independent Hermite polynomials of the white-noise function $a(\xi)$. $a(\xi)$ equals $H^{(1)}(\xi)$, is Gaussian, satisfies $\langle a(\xi)\, a(\eta)\rangle = \delta(\xi-\eta)$, and enters the dynamical problem through the initial condition

$$u(x,0) = \int_{-\infty}^{\infty} K_0^{(1)}(x-\xi)\, a(\xi)\, d\xi. \tag{1.4}$$

The velocity is thereby assumed to be Gaussian at time zero, and subsequent departures from Gaussianity are supposed, in some sense, to be small. Meecham truncates (1.3) under the assumptions that Gaussianity introduced at the beginning dominates the decaying turbulence throughout its lifespan, and that the higher-order terms in (1.3) are necessarily small for a nearly Gaussian u.

2. Numerical solutions for a truncated expansion of the Burgers equation

The Burgers equation is

$$\frac{\partial u}{\partial t} + u\frac{\partial u}{\partial x} = \nu\frac{\partial^2 u}{\partial x^2}, \tag{2.1}$$

where ν is the kinematic viscosity. The Wiener–Hermite expansion of (2.1) involves three steps. First, $u(x,t)$ is replaced with the expansion (1.3). Secondly, the resulting expression is multiplied by any one of the Hermite polynomials of the white-noise function. Thirdly, the product is averaged over the ensemble of white-noise functions. The ensemble average projects (2.1) onto the statistically orthogonal Hermite polynomials of the white-noise function in the same way that a spatial integration projects (2.1) onto sines and cosines in an inverse Fourier transformation. Those three steps extract an equation for the time derivative of the kernel that appears in (1.3) as the coefficient of the particular Hermite polynomial used in the second step. Applied to each Hermite polynomial in turn, the extraction process generates an infinite set of coupled equations for the evolution of the infinite set of kernels in (1.3). Randomness is thereby removed from the problem at the outset, and one can concentrate on finding approximate solutions for the kernels. It is important to recall that the kernels account for the time dependence of the flow as well as for its statistical properties. The infinite bank of equations for the kernels contains exactly the same information as the Burgers equation. If all the kernels were known, then exact solutions of the Burgers equation could be recovered from the expansion (1.3).

The Wiener–Hermite expansion is computationally useless unless it can be truncated after a very few terms. Meecham ignores all but the first two terms in (1.3) and arrives at a pair of coupled integro-differential equations for $K^{(1)}$ and $K^{(2)}$. The Fourier-transformed versions of the equations are simpler and can be solved more accurately than the original equations in physical space. Transformations carried out according to Meecham's convention, for example

$$K^{(1)}(k) = \int_{-\infty}^{\infty} K^{(1)}(x)\, e^{ikx}\, dx,$$

yield the following pair of equations:

$$\left\{\frac{\partial}{\partial t} + \nu k^2\right\} K^{(1)}(k) = \frac{ik}{\pi} \int_{-\infty}^{\infty} K^{(1)}(m)\, K^{(2)}(-m, k)\, dm, \tag{2.2}$$

and

$$\left\{\frac{\partial}{\partial t} + \nu(k+l)^2\right\} K^{(2)}(k,l) = \frac{i}{2}(k+l)\, K^{(1)}(k)\, K^{(1)}(l) + \frac{i}{\pi}(k+l) \int_{-\infty}^{\infty} K^{(2)}(m,k)\, K^{(2)}(-m,l)\, dm \tag{2.3}$$

(Jeng, Foerster, Haaland & Meecham 1966). The two kernels make separate contributions to the energy spectrum $\mathscr{E}(k,t)$. Thus

$$\mathscr{E}(k,t) = \mathscr{E}_1(k,t) + \mathscr{E}_2(k,t), \tag{2.4}$$

where

$$\mathscr{E}_1 = \frac{1}{2\pi} |K^{(1)}(k)|^2, \tag{2.5}$$

and

$$\mathscr{E}_2 = \frac{1}{2\pi^2} \int_{-\infty}^{\infty} |K^{(2)}(m, k-m)|^2\, dm. \tag{2.6}$$

The spectrum is normalized so that the quantity

$$E(t) = \int_0^{\infty} \mathscr{E}(k,t)\, dk$$

equals the total mean energy density $\langle \frac{1}{2}u^2 \rangle$. E is likewise a sum of distinct contributions E_1 and E_2 from the two kernels. The size of the ratio E_2/E_1 is the best available indication of how fast a Wiener–Hermite expansion converges.

We have solved equations (2.2) and (2.3) numerically for a range of Reynolds numbers, and we present typical histories of E and its components E_1 and E_2 in figures 1 and 2. Each numerical experiment begins with the spectrum

$$\mathscr{E}_0(k) = \frac{16}{3}\sqrt{\left(\frac{2}{\pi}\right)} U^2 L (kL)^4 e^{-2(kL)^2}, \tag{2.7}$$

where U is the root-mean-square velocity $\sqrt{\langle u^2 \rangle}$, and the length scale L is the inverse of the wave-number at which $\mathscr{E}_0(k)$ has its maximum. Following Meecham, we assume that the flow is originally Gaussian so that, as far as (2.2) and (2.3) are concerned, the initial conditions are

$$K_0^{(1)}(k) = 4(\tfrac{2}{3})^{\frac{1}{2}} (2\pi)^{\frac{1}{4}} U L^{\frac{1}{2}} (kL)^2 e^{-(kL)^2}, \tag{2.8}$$

from (2.5), and

$$K_0^{(2)}(k, l) = 0.$$

The calculations involved step-function approximation for the kernels, with ten steps per wave-number interval $2L^{-1}$, the interval spanned by the initial spectrum (2.7).

The initial energy spectrum (2.7) differes from the bell-shaped spectrum used by Meecham and his co-workers (Meecham & Siegel 1964, Jeng *et al.* 1966). We chose (2.7) so that the integral of the initial correlation function $R_0(r)$, namely

$$\int_{-\infty}^{\infty} R_0(r)\, dr = \mathscr{E}_0(0),$$

would be zero. If it were non-zero, then a region of length $\mathscr{L}$ spanning many eddies would contain a net momentum proportional to $\sqrt{\mathscr{L}}$; Saffman (1967) has discussed the analogous situation in three dimensions. A momentum growing as $\sqrt{\mathscr{L}}$ is mathematically possible, but the result is a meandering function $u(x, t)$ that conflicts with one's intuitive picture of Burgers's model turbulence. The turbulence corresponding to (2.7) is more nearly analogous to three-dimensional turbulence produced by wind-tunnel grids, since they cannot impart arbitrarily large momenta either.

It is convenient to discuss the figures in terms of an initial Reynolds number

$$R = UL/\nu$$

and a time scale

$$T = L/U,$$

which, at high Reynolds numbers, is roughly the time that elapses before strong shocks form.

The ratio E_2/E_1 remains small over the whole decay period for Reynolds numbers about 2 or below, so succeeding terms in the Wiener–Hermite expansion may indeed be small. The cases $R \lesssim 2$ are not stringent tests, however, because the Burgers equation behaves almost linearly at such low Reynolds numbers. Figure 1 shows the history of the energy at a Reynolds number of 5. The heavy line is a plot of E/E_0 against t/T, where the subscript 0, as usual, denotes conditions at time zero. The finer curves, which are plots of E_1/E_0 and E_2/E_0, show

how the energy is partitioned between the two kernels. E_2 becomes larger than E_1 at $t = 1{\cdot}8T$. Equations (2.2) and (2.3), after that time, probably represent the dynamics badly. The bulk of the energy resides in the second kernel, and it is safe to assume that higher-order kernels would be significantly excited if they were admitted into the computations.

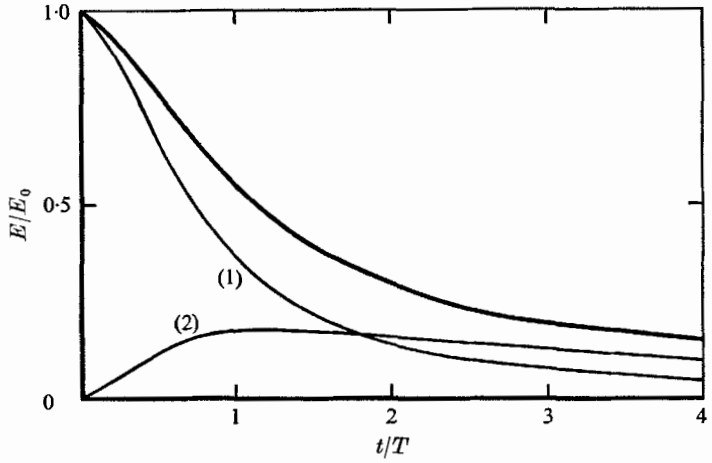

FIGURE 1. Energy history computed from equations (2.2) to (2.6). $R = 5$.

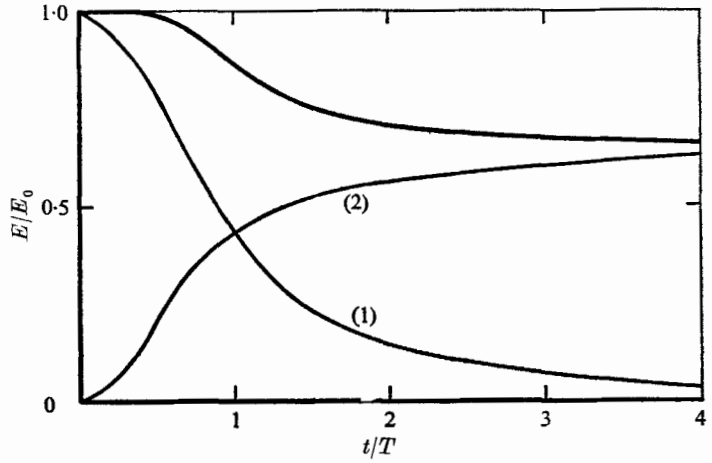

FIGURE 2. Energy history computed from equations (2.2) to (2.6). $R = 20$.

Figure 2 shows the energy histories at $R = 20$. E_2 exceeds E_1 by the time $t = 1{\cdot}0T$. Moreover, only 32 % of the net energy has been dissipated up to the time $t = 4{\cdot}0T$ when the calculations end. That is completely inconsistent with the behaviour of the Burgers equation itself (figure 5 shows the results of numerical experiments on the Burgers equation; for $R = 20$ and $t = 4{\cdot}0T$, the energy has decayed down to 18 % of its initial value). Equations (2.2) and (2.3) grossly underestimate the rate of energy decay at moderately high Reynolds numbers.

The reason that they do so is explained in the next section: the equations contain no convolution integrals and, as a consequence, cannot cascade energy into the dissipation range.

3. Inability of a truncated Wiener–Hermite series to represent an energy cascade

The Fourier transform of the Burgers equation (2.1) is

$$\left\{\frac{\partial}{\partial t}+\nu k^2\right\} b(k) = \frac{i}{2\pi}\int_{-\infty}^{\infty} m b(m)\, b(k-m)\, dm, \tag{3.1}$$

where $b(k)$ is the velocity field transformed according to Meecham's convention. The convolution integral appearing in (3.1) is the Fourier-transformed advection term $u\,\partial u/\partial x$. The convolution integral allows distant Fourier modes to interact. If the energy spectrum is initially localized in a particular region of wave-number space, then the convolution integral rapidly carries energy to other regions.

Both (2.2) and (2.3) contain terms associated with the advection process, but those terms are fundamentally unlike the right-hand side of (3.1): they are free of convolutions. The following example shows how the absence of convolutions blocks the energy cascade. Suppose that, at time zero, $K^{(2)}(k,l)$ is zero everywhere and $K^{(1)}(k)$ is also identically zero for $|k|$ greater than some $k_{\max}$. After a short time δt, according to (2.3), the second kernel will have attained a value

$$K^{(2)}(k,l) = \tfrac{1}{2} i\,\delta t(k+l)\, K_0^{(1)}(k)\, K_0^{(1)}(l), \tag{3.2}$$

which is non-zero only for $|k| \leqslant k_{\max}$ and $|l| \leqslant k_{\max}$. At time δt, therefore, the second kernel is confined in wave-number space to a square whose boundaries are $k = \pm k_{\max}$ and $l = \pm k_{\max}$. Let us consider the effect that the confinement of $K^{(2)}$ has on the evolution of $K^{(1)}$, which satisfies (2.2). At time δt, the transfer term on the right-hand side of (2.2) is still zero for $|k| > k_{\max}$, because $K^{(2)}(-m,k)$ is zero for such values of k. In order for the transfer term in (2.2) to cascade energy to $|k| > k_{\max}$, the second kernel would have to escape from the square to which it is confined at time δt.

The second kernel, however, can never escape. At time δt, the first kernel is still zero for $|k| > k_{\max}$, and it has not begun to grow. The source term in (2.3), the first term on the right, continues to be confined to the original square. The transfer term in (2.3), the second term on the right, is likewise zero for wave-numbers outside the square: for $|k| > k_{\max}$, $K^{(2)}(m,k)$ is zero, and, for $|l| > k_{\max}$, $K^{(2)}(-m,l)$ is zero. At this point, the argument becomes cyclic. The first kernel is trapped on a line interval for all time, and the second kernel is trapped in a square. The kernels cannot flow across their boundaries. Energy simply shuffles from element to element of the two kernels, and all the while they remain within the boundaries imposed at time zero.

Although convolution integrals do not appear in (2.2) and (2.3), one *does* appear in the definition (2.4) of the spectrum $\mathscr{E}(k,t)$. Since $K^{(1)}$ is confined to the interval $|k| \leqslant k_{\max}$, equation (2.5) shows that $\mathscr{E}_1$ is similarly confined. It is

evident from (2.6), however, that $\mathscr{E}_2$ can be non-zero in a larger interval, namely $|k| \leqslant 2k_{\max}$. The spectral band $k_{\max} \leqslant k \leqslant 2k_{\max}$ becomes excited, but $2k_{\max}$ persists as the absolute upper limit for all time. If $2k_{\max}$ falls short of the dissipation range of wave-numbers, then equations (2.2) and (2.3) cannot dissipate energy realistically.

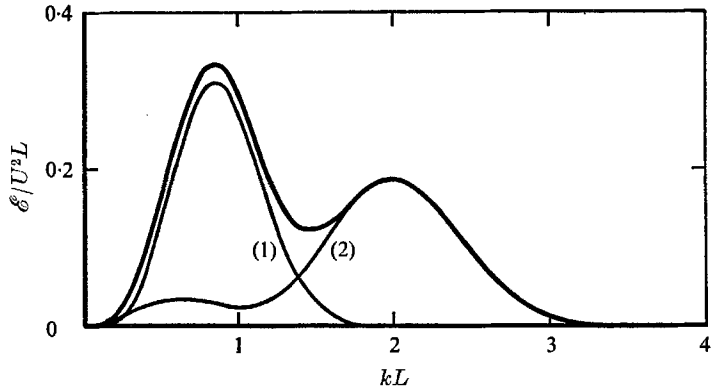

FIGURE 3. Energy spectrum computed from equations (2.2) to (2.6). $R = 20$ and $t = 1{\cdot}0T$. The heavy curve is $\mathscr{E}/U^2L$, the curve labelled (1) is $\mathscr{E}_1/U^2L$, and the curve labelled (2) is $\mathscr{E}_2/U^2L$.

The argument so far has been presented in terms of a kernel $K^{(1)}(k)$ whose initial value is identically zero for $|k| > k_{\max}$. The conclusion that (2.2) and (2.3) fail to cascade energy applies just as well, nevertheless, to an initial kernel of the type (2.8). Figure 3 shows the energy spectrum and its partition between the first and second kernels computed from equations (2.2)–(2.6) for a Reynolds number of 20. Figure 3 is based on the same numerical experiment as figure 2 and shows the spectrum at a time $t = 1{\cdot}0T$ when, according to figure 2, the quantities E_1 and E_2 are about equal. The total spectral distribution $\mathscr{E}/U^2L$ is plotted against the dimensionless wave-number kL as a heavy line, and the components $\mathscr{E}_1/U^2L$ and $\mathscr{E}_2/U^2L$ are plotted as finer lines. It is clear that the wave-number $2L^{-1}$, beyond which the initial spectrum (2.7) is essentially zero, is acting as an effective $k_{\max}$. $\mathscr{E}_1$ is trapped below $2L^{-1}$, and its shape is qualitatively similar to its original shape (2.7), that is, roughly symmetric around L^{-1}. $\mathscr{E}_2$ has spread out twice as far, but is trapped below $4L^{-1} \approx 2k_{\max}$ just as the argument of the previous paragraph would suggest. $\mathscr{E}_2$ is nearly symmetric around its midpoint $2L^{-1}$. It is shaped much like $\mathscr{E}_1$, in fact, except for a tail extending to low wave-numbers. For small times, at least, it is easy to show analytically how that comes about. Equation (3.2) gives $K^{(2)}$ at a time δt. According to (2.5) and (2.6), therefore,

$$\mathscr{E}_2(k, \delta t) = \frac{(\delta t)^2}{2} k^2 \int_{-\infty}^{\infty} \mathscr{E}_0(m)\, \mathscr{E}_0(k-m)\, dm.$$

If $\mathscr{E}_0(k)$ is sharply peaked around its maximum at $k = L^{-1}$, then the integral can be evaluated explicitly:

$$\mathscr{E}_2(k, \delta t) = \frac{(kU\,\delta t)^2}{2} \{\mathscr{E}_0(k-L^{-1}) + \mathscr{E}_0(k+L^{-1})\}. \tag{3.3}$$

The expression inside the brackets has sharp peaks at the three wave-numbers $k = 0, \pm 2L^{-1}$, but because of the factor k^2 in front $\mathscr{E}_2$ is sharply peaked at $k = \pm 2L^{-1}$. Thus $\mathscr{E}_2$ has its strong maxima at twice the wave-numbers $\pm L^{-1}$ characterizing the maxima of $\mathscr{E}_1$. Figure 3 indicates that that condition persists up to times of order T.

The conclusion that $K^{(1)}$ is trapped on a line interval and $K^{(2)}$ is trapped in a square remains valid even when more than two terms are included in the Wiener–Hermite expansion (1.3). Siegel, Imamura & Meecham (1965) have presented the general equation for the time development of the kernels. At no level of truncation are convolution integrals introduced. If three terms are included in the expansion, for example, and if $K^{(1)}$ is initially confined to the interval $|k| \leqslant k_{\max}$, then the arguments of this section can be extended to show that, *for all time*, $K^{(1)}(k)$ is confined to that interval, $K^{(2)}(k, l)$ is confined to a square $|k|, |l| \leqslant k_{\max}$, and $K^{(3)}(k, l, m)$ is confined to a cube $|k|, |l|, |m| \leqslant k_{\max}$. The three kernels are so confined no matter how many terms are included in the expansion, and subsequent kernels are confined to higher-dimensional analogues of the cube. We conclude that the inability of the kernels to escape their boundaries in wave-number space is a fundamental attribute independent of the order of truncation and is therefore an exact consequence of the Burgers equation.

Suppose a third term were included in the Wiener–Hermite expansion. The spectrum $\mathscr{E}$ would then be a sum of three terms, $\mathscr{E}_1+\mathscr{E}_2+\mathscr{E}_3$, where $\mathscr{E}_1$ and $\mathscr{E}_2$ still satisfy (2.4) and (2.5), and

$$\mathscr{E}_3 = \frac{6}{(2\pi)^3}\int\int_{-\infty}^{\infty} |K^{(3)}(l, m, k-l-m)|^2\, dl\, dm.$$

$\mathscr{E}_3(k, t)$ can be non-zero out to $3k_{\max}$, since $K^{(3)}(k_{\max}, k_{\max}, 3k_{\max}-k_{\max}-k_{\max})$ need not be zero. Including a third term in the expansion adds a third band to the range of accessible wave-numbers. By the same kind of argument that led to (3.3), moreover, it is easy to show that $\mathscr{E}_3$ is more-or-less peaked around $k = 3L^{-1}$. The discussion can be extended to cover as many terms in the Wiener–Hermite expansion as desired. Figure 4 is a sketch of what might happen if *all* the terms were included in the expansion of a relatively low Reynolds number velocity field. Roughly speaking, the Nth kernel contributes the portion of the spectrum $\mathscr{E}(k, t)$ near $k = NL^{-1}$. Successive terms in the Wiener–Hermite expansion are associated with successive bands in wave-number space. An expansion comprising N terms can account for dissipation only if

$$NL^{-1} \sim k_{\text{diss}} \sim RL^{-1}.$$

Thus N must be about as large as the Reynolds number of the turbulence. The Wiener–Hermite expansion based on the initial state of the flow is therefore a useless representation at high Reynolds numbers.

Meecham & Siegel (1964) start from a two-term expansion and formulate a theory that does allow an energy cascade. The cascade originates after they make several approximations, one of which changes the fundamental structure of the theory and gives rise to results qualitatively inconsistent with the original equations (2.2) and (2.3). They drop the second term on the right of (2.3) and

assume that (3.2) is always an adequate approximation, provided δt is replaced with T. A simple equation relating the energy spectrum $\mathscr{E}$ to its Gaussian component $\mathscr{E}_1$ results:

$$\left\{\frac{\partial}{\partial t}+2\nu k^2\right\}\mathscr{E}(k,t) = Tk^2\int_{-\infty}^{\infty}[\mathscr{E}_1(k-m,t)\,\mathscr{E}_1(m,t)-2\mathscr{E}_1(k,t)\,\mathscr{E}_1(m,t)]\,dm. \quad (3.4)$$

Meecham & Siegel then close (3.4) by replacing $\mathscr{E}_1$ with $\mathscr{E}$ under the transfer integral and thereby release an open-ended cascade. $\mathscr{E}(k,t)$ evolves into the k^{-2} spectrum characteristic of shock discontinuities (Saffman 1968). The k^{-2} spectrum should not be counted as an argument for truncated Wiener–Hermite expansions, however, because the closed version of (3.4) follows more naturally from the straightforward quasi-normal theory of Reid (1956).

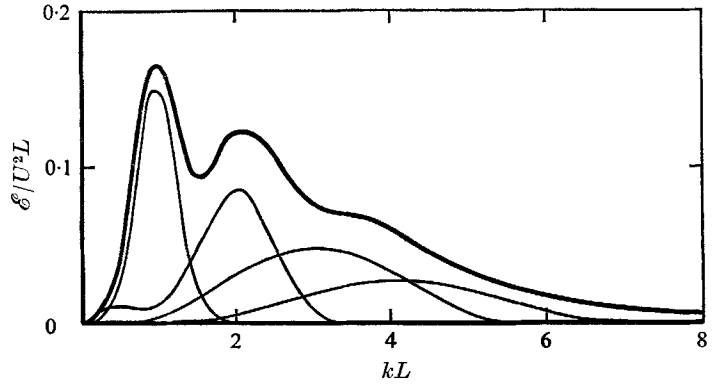

FIGURE 4. Sketch of a possible energy spectrum for the model turbulence. Contributions from the first four Wiener–Hermite kernels are shown as fine lines. The heavy line is the total spectrum.

4. Numerical analysis of turbulence into Gaussian and non-Gaussian components

We showed in the previous section that the first term of the Wiener–Hermite expansion (1.3) cannot help to represent an energy cascade. The argument, set in wave-number space, was rather formal. In this section, we describe results obtained directly from numerical experiments on the Burgers equation (2.1). The results provide a simple physical explanation of why the Gaussian component of turbulence cannot participate in a cascade.

A great deal is known about random solutions of the Burgers equation in physical space, and Saffman (1968) has reviewed the subject recently. At low Reynolds numbers, for example, the advection term in (2.1) is negligible, the turbulence decays by viscous diffusion, and the energy decreases algebraically with time. For an initial spectrum of the form (2.7),

$$\frac{E}{E_0} = \left(1+\frac{t}{RT}\right)^{-\frac{5}{2}}. \quad (4.1)$$

The relaxation time is RT.

At high Reynolds numbers, on the other hand, shocks form out of an originally Gaussian flow in a time of order T. The spectrum (2.7) is sharply peaked around its maximum at $k = L^{-1}$, so the corresponding initial fields $u(x, 0)$ are roughly periodic at a wavelength $\lambda = 2\pi L$. If an initial field were exactly sinusoidal, with a wavelength λ and a root-mean-square amplitude U, then shocks would form at $t = 0{\cdot}71T$ and reach their maximum intensity at $t = 1{\cdot}11T$. The time scales for the formation of strong shocks under random initial conditions are about the same.

Little energy is dissipated at high Reynolds numbers until the shocks form. Having formed, however, the shocks dissipate energy at a rate controlled by large-scale, triangular eddies (cf. figure 7). The eddies relax in a time of order T, regardless of the Reynolds number as long as it is large. The eddies, as they relax, advect their energy into adjacent shocks whose thicknesses adjust to dissipate the energy as it comes. If the eddy field consisted of regular saw-tooth elements of length λ and maximum amplitude U, then the velocity would jump from U to $-U$ across shocks of thickness

$$\delta = \frac{2L}{R} \ln (2\pi R), \tag{4.2}$$

measured from a maximum of u to the minimum immediately following. Increasing the Reynolds number merely decreases the thickness of the shocks; it cannot alter the large-scale structure of the eddies or the rate at which they relax. For a given initial spectrum, therefore, energy decay curves obtained from the Burgers equation must approach a definite limiting shape as $R \to \infty$.

We carried out our numerical experiments on a CDC-3400 computer. The computer started by setting up Gaussian initial conditions according to equation (1.4). The inverse transform of (2.8),

$$K_0^{(1)}(x) = \left(\frac{2}{3}\right)^{\frac{1}{2}} \left(\frac{2}{\pi}\right)^{\frac{1}{4}} UL^{-\frac{1}{2}} \left[1 - \frac{1}{2}\left(\frac{x}{L}\right)^2\right] e^{-(x/2L)^2},$$

was chosen for the initial kernel. That choice makes the results of this section comparable to those of § 2. The white-noise function $a(\xi)$ was approximated by a step-function whose elements were assigned independent, Gaussianly distributed pseudo-random values. Having established the initial condition, the computer traced the evolution of $u(x, t)$ by means of a finite-difference approximation to (2.1), namely the quadratic advection scheme discussed by Leith (1965).

Two length scales characterize the numerical programme: a step-length Δx, and the length $\mathscr{L}$ of the strip of evolving turbulence. The same step-length was used for the step-function approximation to $a(\xi)$ and for the finite-difference solution of the Burgers equation. For high Reynolds number problems, the step-length was chosen so that strong shocks spanned about four steps: $\Delta x \approx \frac{1}{4}\delta$. That kept the computations sufficiently accurate, and, at the same time, ensured that the approximate $a(\xi)$ was sufficiently white. The length scale $\mathscr{L}$ was made as large as possible so that ensemble averages could be estimated accurately as spatial averages over $\mathscr{L}$. Since the computer could handle internally at most 5000 grid points, $\mathscr{L}$ was always $5000\Delta x$. At a Reynolds number of 5, for example, $3\frac{1}{3}$ steps were used in each interval L. A typical eddy, having a length λ,

therefore spanned about 20 grid points. The length $\mathscr{L}$ of the strip of turbulence was $1500L$ or about 240λ. At a Reynolds number of 20, $\mathscr{L}$ had to be less than 100λ. Since the number of roughly independent eddies was of the order of 100, the fractional error expected of spatial averages is about $\sqrt{(100)}/100$, or 10 %.

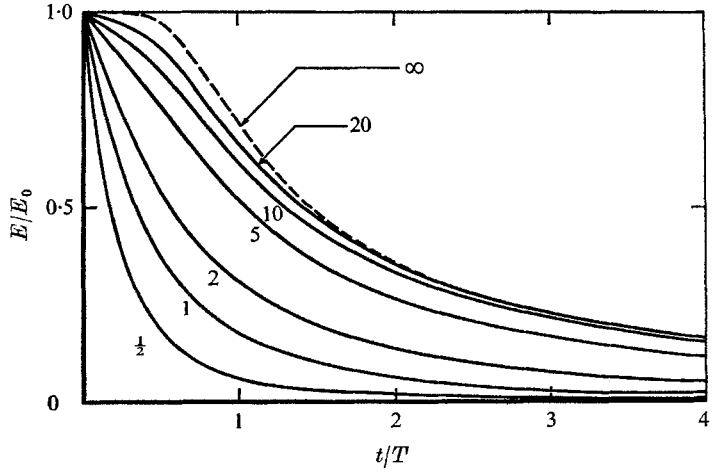

FIGURE 5. Energy decay curves computed directly from the Burgers equation. Reynolds numbers are shown inside the figure. The dotted line, obtained by extrapolation, is the asymptotic decay profile for $R \to \infty$.

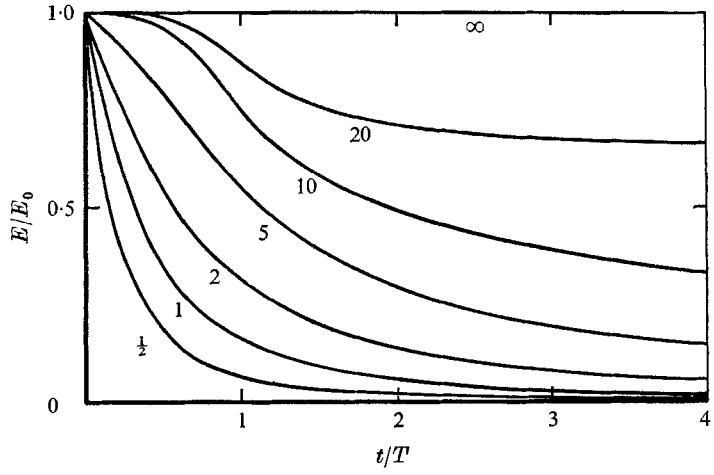

FIGURE 6. Energy decay curves computed from equations (2.2) to (2.6).

Having determined $u(x, t)$, the computer estimated the energy E by averaging $\frac{1}{2}u^2$ over the interval $\mathscr{L}$. The estimate has an expected error of 10 %. $E(t)$ and its initial value E_0 should be off by about the same percentage, however, so a plot of $E(t)/E_0$ should be quite accurate. Figure 5 shows a family of such decay curves obtained from the numerical experiments on the Burgers equation; E/E_0

is plotted against t/T for Reynolds numbers of $\frac{1}{2}$, 1, 2, 5, 10, and 20. The curves obtained at $R = \frac{1}{2}$ and 1 follow the law for linear relaxation, equation (4.1), very closely. The curve at $R = 2$ drops somewhat faster than (4.1) predicts, and the curve at $R = 5$ drops much faster. Strong shocks form when $R = 5$ (cf. figure 7), and non-linear advection, rather than viscous diffusion, controls the rate of decay. The decay curve changes very little as R increases from 5 to 10, and still less from 10 to 20. The dotted curve represents the limiting decay profile for $R \to \infty$. It was obtained from the computed profiles by plotting E/E_0 against $1/R$, for various t/T, and extrapolating the plots to $1/R = 0$. The limiting profile has zero slope at $t/T = 0$. A Gaussian initial state contains no shocks, and no dissipation can occur at infinite Reynolds number until shocks form.

Figure 6 shows the corresponding decay curves obtained by integrating (2.2) and (2.3). Equation (4.1) and the curves of figures 5 and 6 all agree very well at $R = \frac{1}{2}$ and 1. At $R = 5$, the curve in figure 6 is about 10 % high, and the error grows dramatically for larger Reynolds numbers. Equations (2.2) and (2.3) predict an appreciable decay only after a time of order RT, the linear relaxation time, and they predict no decay at all for $R \to \infty$. The first two terms of the Wiener–Hermite expansion (1.3) cannot represent shocks and therefore cannot account for a relaxation process having a time scale T.

The computer next extracted the kernel $K^{(1)}(x)$ appearing in the Gaussian term of (1.3). In terms of an ensemble average,

$$K^{(1)}(x) = \langle u(x+\xi, t)\, a(\xi)\rangle. \tag{4.3}$$

Because the turbulence is homogeneous, (4.3) is valid for any ξ. For the purposes of numerical computation, of course, (4.3) was approximated by a spatial average over the interval $-\frac{1}{2}\mathscr{L} < \xi < \frac{1}{2}\mathscr{L}$. The error expected of the extraction procedure is again about 10 % at the higher Reynolds numbers. The final stage of the numerical programme was the reconstruction of the Gaussian term of (1.3) itself:

$$u_1(x,t) = \int_{-\infty}^{\infty} K^{(1)}(x-\xi)\, a(\xi)\, d\xi.$$

Figure 7 (*a*) shows a segment of computer-generated turbulence. The Reynolds number is 5, the time t is $1{\cdot}0T$, and the length of the segment is $20L$. The velocity jumps average about $2U$ across the shocks, so (4.2) is applicable. The figure and the equation both indicate that δ and L are about equal. Figure 7 (*b*) shows the Gaussian component u_1 of the same segment of turbulence, and figure 7 (*c*) shows the difference $u - u_1$, which is the sum of all the non-Gaussian components of u. As far as amplitude is concerned, the Gaussian component is dominant. There is a striking qualitative difference between u and u_1, however, and that difference is the basis of the fact that u_1 cannot participate in an energy cascade. The Gaussian function $u_1(x,t)$ is statistically symmetric under a change in sign, whereas $u(x,t)$ is not. The net velocity $u(x,t)$ is statistically symmetric under simultaneous changes in the signs of u and x (that can be seen by inspecting figure 7 (*a*) upside down !), but the shocks face in the wrong direction if the velocity alone changes sign. Because it must remain symmetric, the Gaussian component u_1 cannot follow the total field u as it skews into shocks. The shock structure can be represented

in (1.3) only by properly skewed quadratic and higher-order terms. Figure 7 (*c*) shows that $u - u_1$, the sum of the non-Gaussian terms, is indeed responsible for the shocks. Strong shocks occur at $x/L = 3$, 8, and 16 in figure 7 (*a*), and well-defined velocity couplets occur at those points in figure 7 (*c*). Since the Gaussian component cannot incorporate shocks, it cannot contain high wave-number modes of the Fourier-transformed velocity field. Those modes are associated

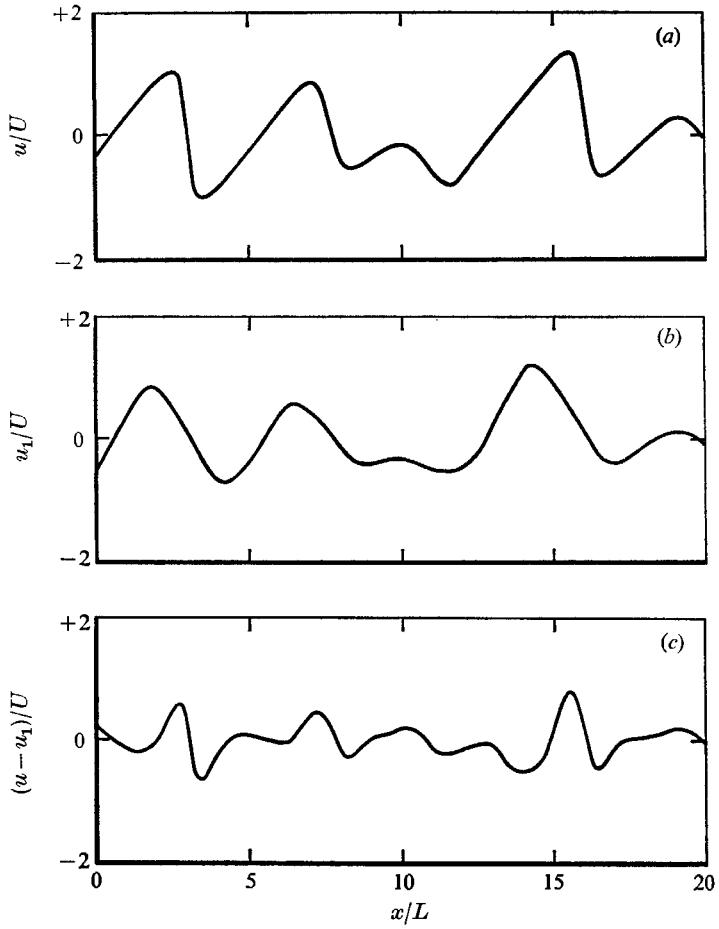

FIGURE 7. (*a*) Segment of the model turbulence at $R = 5$ and $t = 1{\cdot}0T$. (*b*) Gaussian component of the turbulence. (*c*) Sum of the higher-order components.

with the shock structure and therefore with the non-Gaussian component $u - u_1$ of the flow. It is clear from figures 7 (*b*) and (*c*) that the function $u - u_1$ is pitched at a considerably higher wave-number than u_1.

Energy cascade and shock formation are the same process. A cascade of energy does not give rise to jumbled, staccato turbulence, the sort that a high-pitched Gaussian function could represent, but to a sequence of well-spaced shocks. The Gaussian component of the field cannot skew into shocks, so it fails to incorporate them as they form. The Fourier transform of u_1 cannot contain

high wave-number modes, because they are associated exclusively with the shocks. That is the reason $\mathscr{E}_1$, the spectrum of u_1, is confined for all time to low wave-numbers.

5. Conclusions

We have come to the following conclusions:

1. Equations derived by truncating the Wiener–Hermite series (1.3) do not yield a sufficiently rapid energy decay at high Reynolds numbers. For $R \gg 1$, the energy is nearly constant over an eddy time T.

2. The reason that the energy decays so slowly is that there is no mechanism for an energy cascade *within* a low-order term of the Wiener–Hermite expansion. Instead, a cascade of energy through wave-number space corresponds roughly to a cascade of energy through successive terms in the expansion. The kernel $K^{(1)}$ is confined to a definite line-interval in wave-number space *for all time*, $K^{(2)}$ is confined to a square, $K^{(3)}$ to a cube, and so on. A k^{-2} spectrum can be obtained only by means of an approximation that is inconsistent with exact consequences of the theory.

3. The physical reason why $K^{(1)}$ is confined for all time is that the Gaussian part of a random function is statistically symmetric under a change of sign and cannot help to represent shocks. The shock structure, which comprises the high wave-number components of the velocity field, can be represented only by higher-order kernels.

The question remains whether a truncated expansion like (1.3) might represent real hydrodynamic turbulence better than it does the Burgers model. The single-point probability distribution of a three-dimensional turbulent field is indeed nearly Gaussian (Batchelor 1953), and the experimentally observed Gaussianity has been advanced as a justification for truncating Wiener–Hermite expansions (Meecham & Siegel 1964). As far as the experiments are concerned, however, 'Gaussianity' means that velocities measured simultaneously, but at separate points in space, have a joint-normal probability distribution; that property we shall call spatial Gaussianity. A function $u(x,t)$ that has evolved deterministically from a random initial state $u(x,0)$ could be spatially Gaussian to all orders and still require many terms of (1.3) for its representation. The quadratic and higher-order terms in (1.3) can be zero *only if* $u(x,t)$ *and its initial state* $u(x,0)$ *have a joint-normal probability distribution*; we shall call that condition temporal Gaussianity. Non-linearity might create spatial Gaussianity and simultaneously act to destroy temporal Gaussianity.

Let us sharpen that argument by returning to the case, discussed in the introduction, of a simple random variable $y(t;a)$ whose initial value a has a Gaussian probability distribution $G(a)$. Suppose that

$$dy/dt = -2a\,\delta(t-|a|),$$

where δ is the Dirac delta function. The solution bears a highly non-linear relationship to its random initial condition:

$$y(t;a) = \begin{cases} a & \text{if} \quad t < |a|, \\ -a & \text{if} \quad t > |a|. \end{cases}$$

In other words, a system starting at $y(0;a) = a$ flips sign at the instant $t = |a|$. The random variable $y(t;a)$ can be expanded in Hermite polynomial form (1.1), and the coefficients $k_n(t)$ can be extracted by means of (1.2). The expansion begins as follows:

$$y(t;a) = \left[1 - 2\,\mathrm{erf}\left(\frac{t}{\sqrt{2}}\right) + 2\sqrt{\left(\frac{2}{\pi}\right)}\, t \exp\left(\frac{-t^2}{2}\right)\right] h_1(a) + \left[\frac{2}{\sqrt{(3\pi)}}\, t^3 \exp\left(\frac{-t^2}{2}\right)\right] h_3(a) + \ldots.$$

At $t = 0$, $y = h_1(a) = a$. As $t \to \infty$, $y \to -a$, which simply means that at large times almost all the systems have flipped sign and $y(t;a)$ is related linearly again to its initial condition. For t finite, however, all the odd-numbered higher-order terms of the Hermite expansion are excited. $k_1(t)$ passes through zero at one instant, and at that instant y is represented strictly by 'non-Gaussian' terms. Yet, all the while, y remains precisely Gaussian in the sense that its probability distribution is $G(y)$. For every system in the ensemble that flips from $-a$ to a, another flips from a to $-a$, and the probability distribution is unaltered. Gaussianity of y itself implies nothing about the convergence of a Hermite series based on a random initial condition; analogously, spatial Gaussianity of hydrodynamic turbulence, to whatever extent it is present, does not justify truncating a Wiener–Hermite expansion based on the initial state of flow.

The expansion (1.3) is complete, however slowly it converges, but it is not unique. The white-noise function associated with the initial condition (1.4) may not be the best basis for an expansion at a later time. It may be possible to update the white-noise background systematically so that it, rather than the kernels, can represent a chaos developing under non-linear interactions. Wiener (1958) himself recognized that a series of the form (1.3) might not converge rapidly enough, but the chapters in which he proposes an alternative are the most mysterious in his book. The formulation studied in this paper requires that $\partial a(x)/\partial t = 0$; the white noise is an unchanging substratum of the turbulence. Wiener thought that the white noise should be convected by the flow so that $Da(x,t)/Dt = 0$, where D/Dt signifies a convected derivative. It is difficult to accept the claim, however, that a convected function can retain Gaussian characteristics. Several workers recently have tried to build consistent theories using time-dependent white-noise backgrounds (Canavan & Leith 1968, Bodner 1969), and one of those approaches will be discussed in the next paper at this Symposium on Turbulence.

Most of this work was performed in 1967 at the Lawrence Radiation Laboratory, under the auspices of the United States Atomic Energy Commission. We had several stimulating discussions about Wiener–Hermite series with C. E. Leith during that time, and we are grateful. We are indebted further to S. A. Orszag for much helpful criticism during his stay at the Boeing Scientific Research Laboratories.

REFERENCES

BATCHELOR, G. K. 1953 *The Theory of Homogeneous Turbulence.* Cambridge University Press.

BODNER, S. E. 1969 Turbulence theory with a time-varying Wiener–Hermite basis. *Phys. Fluids*, **12**, 33.

CANAVAN, G. H. 1969 A Lagrangian Wiener–Hermite expansion for turbulence. Ph.D. Thesis. University of California at Davis.

CANAVAN, G. H. & LEITH, C. E. 1968 Lagrangian Wiener–Hermite expansion for turbulence. *Phys. Fluids*, **11**, 2759.

JENG, D. T., FOERSTER, R., HAALAND, S. & MEECHAM, W. C. 1966 Statistical initial-value problem for Burgers' model equation of turbulence. *Phys. Fluids*, **9**, 2114.

LEITH, C. E. 1965 Numerical simulation of the earth's atmosphere. *Methods in Computational Physics*, vol. IV. New York: Academic.

MEECHAM, W. C. & SIEGEL, A. 1964 Wiener–Hermite expansion in model turbulence at large Reynolds number. *Phys. Fluids*, **7**, 1178.

MEECHAM, W. C. & JENG, D. T. 1968 Use of the Wiener–Hermite expansion for nearly normal turbulence. *J. Fluid Mech.* **32**, 225.

ORSZAG, S. A. & BISSONNETTE, L. R. 1967 Dynamical properties of truncated Wiener–Hermite expansions. *Phys. Fluids*, **10**, 2603.

REID, W. H. 1956 On the transfer of energy in Burgers' model of turbulence. *Appl. Sci. Res.* A **6**, 85.

SAFFMAN, P. G. 1967 The large-scale structure of homogeneous turbulence. *J. Fluid Mech.* **27**, 581.

SAFFMAN, P. G. 1968 Lectures on homogeneous turbulence. *Topics in Nonlinear Physics.* New York: Springer.

SIEGEL, A., IMAMURA, T. & MEECHAM, W. C. 1965 Wiener–Hermite expansion in model turbulence in the late decay stage. *J. Math. Phys.* **6**, 707.

SIEGEL, A. & MEECHAM, W. C. 1959 *Bull. Am. Phys. Soc. Ser. II*, **4**, 197.

WIENER, N. 1939 The use of statistical theory in the study of turbulence. *Fifth International Congress for Applied Mechanics.* New York: John Wiley.

WIENER, N. 1958 *Nonlinear Problems in Random Theory.* Massachusetts Institute of Technology Press.